Journal of Solid State Chemistry **145,** 655–667 (1999)
Article ID jssc.1999.8277, available online at http://www.idealibrary.com on IDEAL®

Thermal and Structural Investigations of the Bis-Dihexadecyldimethylammonium Dichromate

Nathalie Fosse and Luc Brohan[1]

Institut des Matériaux de Nantes, Laboratoire de Chimie des Solides-CNRS UMR 6502, 2, rue de la Houssinière, BP 32229, 44322 Nantes Cedex 3, France

Received December 3, 1998; in revised form March 1, 1999; accepted March 11, 1999

New mesostructured bis-dialkyldimethylammonium-dichromate of formula $[(C_{16}H_{33})_2(CH_3)_2N]_2Cr_2O_7$ was prepared at 80°C from an aqueous solution of hexadecyldimethylammonium salt and potassium dichromate. Phase transitions have been evidenced by means of thermogravimetric analysis coupled with differential scanning calorimetry and by optical microscopy. As suggested by a preliminary powder X-ray diffraction study, the compound exhibits a lamellar structure. The detailed conformation and molecular packing of the compound were determined from single crystal X-ray diffraction data analysis. $[(C_{16}H_{33})_2(CH_3)_2N]_2Cr_2O_7$ crystallizes in the triclinic system ($P1$ space group, $Z = 1$), with cell parameters $a = 34.330(7)$ Å, $b = 7.800(2)$ Å, $c = 7.250(1)$ Å, $\alpha = 103.69(3)^\circ$, $\beta = 89.86(3)^\circ$, $\gamma = 94.12(3)$. The structure consists of discrete dichromate anions, statistically distributed in a layer, separated by a double-layer of dihexadecyldimethylammonium cationic molecules in which the alkyl chains are lying in parallel. The hydrocarbon chains packing can be described using a triclinic subcell with dimensions $a_s = 5.01$ Å, $b_s = 7.80$ Å, $c_s = 2.57$ Å, $\alpha_s = 90.9^\circ$, $\beta_s = 98.9^\circ$, $\gamma_s = 104.0^\circ$. The packing cross-section of the hydrophilic part is 54.9 Å^2 per molecule of surfactant in the layer plane. Therefore, the chains axis forms a tilt angle of 46° ($\cos\varphi = (a_s \times b_s \times \sin\gamma_s)/a \times b \times \sin\gamma$) relative to the normal of the polar plane.

Key Words: **liquid-crystal phase transitions; chromium oxides; surfactants.**

INTRODUCTION

The synthetic dialkylammonium bromide surfactants, $[(C_nH_{2n+1})_2(CH_3)_2N]^+Br^-$, with bilayer structures have been studied by electron microscopy (1, 2), differential scanning calorimetry, and X-ray diffraction analysis (3), and the similarity of the molecular assembly of these compounds to those of phospholipids found in biological membranes has been shown. The cooperative assembly of such amphiphilic molecules and inorganic structures has been used to prepare a new class of mesoporous aluminosilicate materials which has attracted great interest to catalysis because of their large and uniform distribution of pore sizes (20–100 Å) (4–18). Recently, surfactant molecules have been used as templating agents for mesostructured solids with transition metal oxides (19, 21). Due to a wide range of promising potential applications in adsorption, batteries, catalysis, ceramic precursors, nonlinear optics, electronic conductivity and sensors, interest in transition metal oxides possessing a micro(meso)porous texture or micro(meso) structure[2] has increased over the past few years. With these interests in mind, lamellar mesostructured alkyltrimethylammonium dichromates $(C_nH_{2n+1}(CH_3)_3N)_2\ Cr_2O_7 \cdot xH_2O$ ($n = 12, 14, 16, 18$; $x = 0, 2$) prepared from a mixture of chromium oxide and alkyltrimethylammonium bromide have been recently published (22, 23). In the present paper, we report on the synthesis and characterization of a new anhydrous bisdihexadecyldimethylammonium dichromate (DHDDMACr) by means of thermal analysis, polarizing microscopy, and X-ray diffraction.

EXPERIMENTAL SECTION

As for the bis-alkyltrimethylammonium dichromate salts synthesis (23), the bisdihexadecyldimethylammonium dichromate has been prepared by using a quaternary alkylammonium salt, $[(C_{16}H_{33})_2(CH_3)_2]N^+Br^-$, commercially available from Aldrich Chemical Company. The inorganic reactant was potassium dichromate ($K_2Cr_2O_7$, Merck 99% +). A solution of $K_2Cr_2O_7$, $[(C_{16}H_{33})_2(CH_3)_2]N^+Br^-$ and H_2O in a 1:2:100 molar ratio was heated at 80°C for 48 hours, in a screw top tube. After cooling, the orange solid product was recovered by filtration, washed

[1]To whom correspondence should be addressed.

[2]The terms microstructured, mesostructured, and macrostructured are used analogously to scale definitions for the three classes of porous materials defined by IUPAC (18): First, microporous materials, in which the pore diameter $d_p < 2$ nm; second, mesoporous materials, in which $2\text{ nm} < d_p < 50$ nm; and, third, macroporous materials, in which $d_p > 50$ nm.

0022-4596/99 $30.00

with distilled water, and dried under air at room temperature or at 110°C. The chemical reaction can be summarized as follows:

$$2(C_{16}H_{33})_2(CH_3)_2N^+,Br^- + K_2Cr_2O_7$$

$$\rightarrow [(C_{16}H_{33})_2(CH_3)_2N]_2Cr_2O_7 + 2KBr.$$

Thermal Analysis

Simultaneous thermogravimetric analysis (TGA) and differential scanning calorimetry (DSC) were performed on a SETARAM TG-DSC 111, with heating rate of 5°C min^{-1} under flowing argon. Approximately 20 mg of ground sample was accurately weighed and placed in a platinum sample holder.

Optical Microscopy

The experiments were carried out using a Leitz Orthoplan polarizing microscope, equipped with a programmed temperature stage. A small amount of the sample dispersed in water is placed between the slide and the cover-slip.

Powder X-Ray Diffraction (XRPD)

Powder patterns were collected on a SIEMENS D5000 diffractometer (Cu$K\alpha$ radiation, $\lambda = 1{,}54178$ Å) in a Bragg–Brentano geometry. The step size was 0.03° with a step time of 1.5 s. Diffraction peak positions and integrated intensities were determined using the PROLIX (24) program.

Single Crystal X-Ray Diffraction

Lattice parameters and diffraction intensities were measured on a STOE Imaging Plate Diffraction System diffractometer with filtered Mo$K\alpha$ radiation ($\lambda = 0.710069$ Å). The lattice parameters were refined by the least squares refinement, using 5000 reflections in the θ range of 1.78°–23.82°. The structural solution was solved by a combination of direct methods and Fourier syntheses using XS and XL routines of the SHELXTL software (25) Version 5.

Density Measurement

Density measurement was performed on a (ACCUPYC 1330) micromeritics automatic pycnometer. On the basis of the measured density and unit cell volume determination, the unit cell contains one $[(C_{16}H_{33})_2(CH_3)_2N]_2Cr_2O_7$ molecule.

RESULTS AND DISCUSSION

Thermal Analysis

The thermal stability of the DHDDMACr dried at 100°C was investigated by means of TGA coupled with DSC. The thermal analysis curves are shown in Fig. 1. Between 200 and 460°C, the DHDDMACr exhibits one important weight loss (marked C). The residual compound identified from its XRPD pattern is the Eskolaïte variety of Cr_2O_3.

As observed for the bis-alkyltrimethylammonium dichromates (23), the complete self combustion of DHDDMACr only occurs under air. In the temperature range of 200 to 300°C, the weight loss (C) associated with the exothermic peak (C′) is due to the surfactant decomposition, by a self-combustion process. This large exothermic peak C′ suggests an oxidation–reduction phenomenon through which gaseous products (evolved gas analysis by mass spectrometry) (23) are formed. With respect to the stoichiometry, the simplified thermal decomposition of $[(C_{16}H_{33})_2(CH_3)_2N]_2Cr_2O_7$ can be represented by the equation

$$[(C_{16}H_{33})_2(CH_3)_2N]_2Cr_2O_7 \xrightarrow{\Delta} N_2 + 4H_2O + 4C_{16}H_{34} + 4C + Cr_2O_3.$$

On the DSC curves (Fig. 1), below 200°C, two endothermic transitions (A′, B′) appear. These endothermic transitions located at 69 and 141°C can be attributed to a phase change from anhydrous crystal to liquid-crystal and from liquid-crystal to liquid, respectively. These phase tansitions were directly evidenced during optical experiments using a polarized light microscopy. As shown in Fig. 2a, the

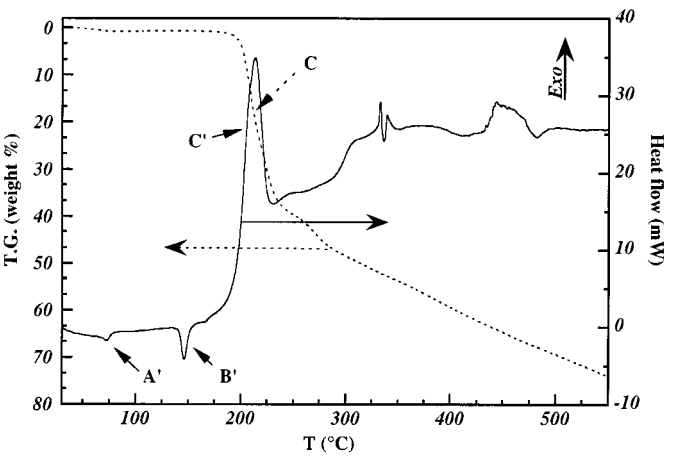

FIG. 1. TG and DSC curves of $[(C_{16}H_{33})_2(CH_3)_2N]_2Cr_2O_7$ dried at 110°C showing two endothermic peaks before the decomposition of the surfactant.

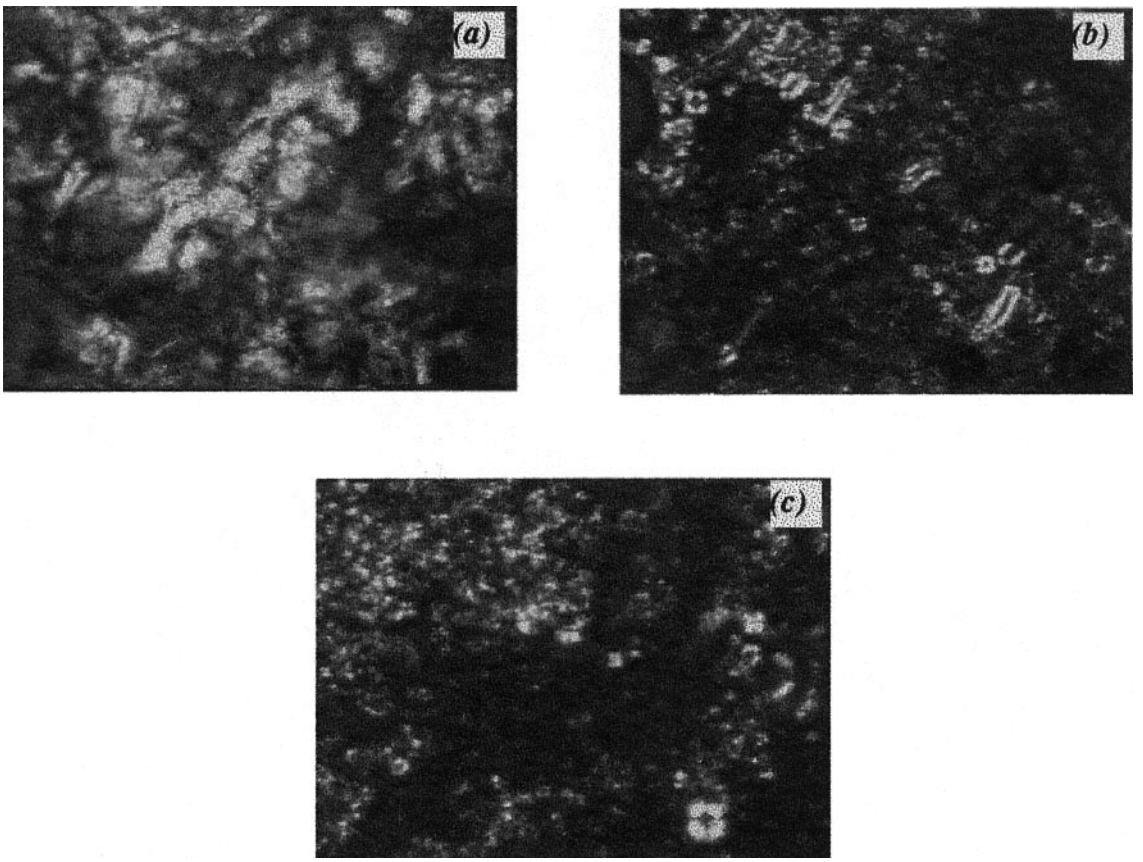

FIG. 2. Polarizing microscope images of anhydrous $[(C_{16}H_{33})_2(CH_3)_2N]_2Cr_2O_7$. (a) Crystal, $T = 25°C$ and optical texture of the mesophase after cooling from isotropic phase at $T = 100°C$ showing oily streaks (b) and a mosaic texture in complex network of positive and negative units (c).

crystallized compound is highly birefringent at room temperature and then a solid-mesophase transition appears near 70°C. In the temperature range 70–140°C, the polarizing microscope images of the bis-dihexadecyldimethylammonium dichromate clearly exhibit common textures encountered in lamellar liquid crystal phases (26). The bright oily streaks (Fig. 2b) and the mosaic texture in a complex network of positive and negative units, observed at $T = 100°C$ (Fig. 2c), are characteristic of a smectic A mesophase.

Structural Characterization

The XRPD patterns of the bis-hexadecyldimethylammonium dichromates dried at room temperature and at 110°C show (Fig. 3) a systematic enhancement of the 00*l* peak intensities due to a preferential orientation. As observed for the monoalkyl dichromates (22), the d_{00l}-spacings (Table 1) are also characteristic of a lamellar structure. The interlayer distance of the DHDDMACr dried at room temperature, refined with the U-FIT program (27), equals 34.116(7) Å, while the interlamellar distance d_{00l} of the DHDDMACr sample heated at 110°C is close to 19.2 Å.

Structure Determination of $[(C_{16}H_{33})_2(CH_3)_2N]_2Cr_2O_7$

X-ray diffraction of $[(C_{16}H_{33})_2(CH_3)_2N]_2Cr_2O_7$ was carried out on an orange plate-shaped single crystal. The data collection conditions are summarized in Table 2. No absorption correction was applied. The structure was solved by a combination of direct methods and Fourier syntheses and applied for $P\bar{1}$ and $P1$ space groups. For the $P\bar{1}$ space group, the chromium atoms' positions and only one planar zigzag alkyl chain position could be readily discerned. In the latter space group, the revealed structure consisted of two amphiphile molecules not related by a center of symmetry, which supported the $P1$ space group for $[(C_{16}H_{33})_2(CH_3)_2N]_2Cr_2O_7$ and only one dichromate group in the unit cell. The positions of the chromium atoms and of three oxygen atoms were determined by a direct method. After several cycles of block-diagonal least squares

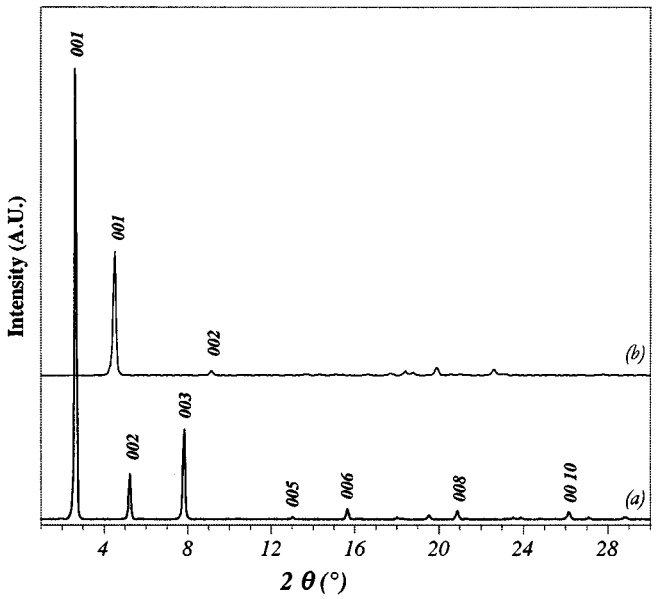

FIG. 3. Powder X-ray diffraction patterns of $[(C_{16}H_{33})_2(CH_3)_2N]_2Cr_2O_7$ dried at (a) room temperature, (b) 110°C.

refinement, there was evidence of nitrogen atoms belonging to the dialkyl chains. Advancing in the resolution of the structure allowed the successive refinement of carbon as well as hydrogen atoms of the dihexadecyldimethylammonium chains. The HFIX subroutine option (riding model) of SHELXTL programs was used for positioning and refining hydrogen atoms. After the refinement of the position parameters, the remaining oxygens in the dichromate group were found from subsequent difference-Fourier maps. Surprisingly, eight oxygen positions appeared in the chromium coordination. After another several cycles including these newly found oxygen atoms, a full matrix least squares calculation was performed to investigate occupancies of oxygen atoms, since the short distances between these oxygen atoms (O1–O8; O3–O9; O4–O10; O7–O11) made it impossible to accommodate each of them simultaneously in the same unit cell. It was found from this calculation that the oxygen atoms with half occupancy were most preferable and they were statistically distributed in an asymmetric unit. At this stage, anisotropic thermal motions of nonhydrogen atoms and hydrogen atoms located on their calculated positions with isotropic temperature factors were included in the refinement, leading to the final $R_{value} = 0.0563$ ($Rw = 0.1288$). The atomic coordinates with isotropic thermal parameters, anisotropic displacement

TABLE 1

h k l	d_{obs} (°)	d_{calc} (°)	Intensity I/I_0
0 0 1	34.1	34.0(1)	100
0 0 2	17.05	17.07(3)	10
0 0 3	11.37	11.37(1)	21
0 0 4	—	—	—
0 0 5	6.823	6.825(5)	1
0 0 6	5.685	5.686(3)	3
0 0 7	—	—	—
0 0 8	4.264	4.264(2)	3
0 0 9	—	—	—
0 0 10	3.411	3.411(1)	2
	refined d_{001} (Å)	34.116(7)	

TABLE 2
Crystal Data, Data Collections, and Refinements of $[(C_{16}H_{33})_2(CH_3)_2N]_2Cr_2O_7$ at 293K

Crystal data	
Chemical formula	$[(C_{16}H_{33})_2(CH_3)_2N]_2Cr_2O_7$
Formula mass (amu)	1205.85
Crystal system	triclinic
Space group	$P1$
Z	1
Radiation	Mo$K\alpha$, $\lambda = 0.7107$ Å
Description	Orange platelike crystal
Size (mm)	$0.3 \times 0.35 \times 0.05$
Temperature	5000 reflections
a (Å)	34.330(7)
b (Å)	7.800(2)
c (Å)	7.250(1)
α (°)	103.69(3)
β (°)	89.86(3)
γ (°)	94.13(3)
V (Å)	1881.1(7)
ρ calc (g.cm^{-3}): 1.064	ρ exp (g.cm^{-3}): 1.089
μ(Mo$K\alpha$) (mm^{-1})	0.335
Data collection	
Diffractometer type	STOE imaging plate
θ range	1.78° to 23.82°
Index ranges	$-38 \le h \le 38$, $-8 \le k \le 8$, $-8 \le l \le 8$
Collected reflections	14641
Independent reflections	10655 [R(Int) = 0.1022]
Observed reflections with $I > 4\sigma(I)$	2686
Refinement (on F^2)	
Atomic scattering factors	Neutral atoms from SHELXTL software
No. of variables	760
$R_1(F)$ [$I > 4\sigma(I)$]	0.0563
w$R_2(F^2)$ [$I > 4\sigma(I)$]	0.1288
$R_1(F)$ for 10655 reflections	0.2304
w$R_2(F^2)$ for 10655 reflections	0.2012
Goodness-of-fit on F^2	0.683
Extinction coefficient	0.0001(3)
Largest diff. peak and hole	0.204 and -0.207 e.Å^{-3}

TABLE 3
Positional Parameters and U(eq) (Å^2) Values for Nonhydrogen Atoms of $[(C_{16}H_{33})_2(CH_3)_2N]_2Cr_2O_7$ at 293K

Atoms	Occupancy	x	y	z	U(eq) (Å^2)
Cr(1)	1	0.8247(1)	0.7694(5)	0.0914(5)	0.085(2)
Cr(2)	1	0.7483(1)	0.4984(5)	− 0.0645(4)	0.087(2)
O(1)	0.5	0.8284(10)	0.862(3)	0.329(3)	0.074(9)
O(2)	1	0.8282(6)	0.903(2)	− 0.028(2)	0.102(8)
O(3)	0.5	0.8461(7)	0.591(3)	0.046(3)	0.085(9)
O(4)	0.5	0.6951(7)	0.538(4)	− 0.030(2)	0.072(8)
O(5)	1	0.7527(5)	0.411(2)	− 0.297(1)	0.084(6)
O(6)	1	0.7449(5)	0.329(1)	0.055(2)	0.082(6)
O(7)	0.5	0.7700(6)	0.686(4)	0.046(4)	0.13(1)
O(8)	0.5	0.8143(8)	0.826(4)	0.279(2)	0.060(8)
O(9)	0.5	0.8759(6)	0.740(3)	0.105(2)	0.060(7)
O(10)	0.5	0.7313(14)	0.663(3)	− 0.001(4)	0.15(1)
O(11)	0.5	0.8029(7)	0.542(2)	− 0.048(2)	0.052(7)
N(1)	1	0.7231(3)	0.929(2)	0.565(1)	0.035(4)
C(100)	1	0.7140(6)	0.729(2)	0.505(3)	0.070(6)
C(101)	1	0.6785(6)	0.664(2)	0.382(2)	0.060(5)
C(102)	1	0.6645(6)	0.483(3)	0.353(3)	0.096(9)
C(103)	1	0.6485(6)	0.428(3)	0.510(3)	0.067(7)
C(104)	1	0.6106(7)	0.503(3)	0.582(3)	0.080(7)
C(105)	1	0.5963(7)	0.450(3)	0.761(3)	0.067(7)
C(106)	1	0.5564(8)	0.511(3)	0.827(3)	0.081(8)
C(107)	1	0.5443(7)	0.460(3)	0.022(3)	0.081(8)
C(108)	1	0.5044(8)	0.515(3)	0.083(3)	0.082(8)
C(109)	1	0.4915(7)	0.458(3)	0.274(3)	0.077(8)
C(110)	1	0.4511(7)	0.509(4)	0.340(3)	0.087(8)
C(111)	1	0.4416(7)	0.445(3)	0.523(3)	0.079(7)
C(112)	1	0.4020(8)	0.492(3)	0.596(3)	0.109(9)
C(113)	1	0.3870(8)	0.430(3)	0.781(3)	0.108(9)
C(114)	1	0.3501(8)	0.494(4)	0.875(3)	0.13(1)
C(115)	1	0.334(1)	0.406(5)	0.025(4)	0.20(1)
C(150)	1	0.7331(6)	0.018(2)	0.406(2)	0.082(7)
C(120)	1	0.7600(5)	0.955(3)	0.720(2)	0.079(6)
C(130)	1	0.6896(7)	0.021(3)	0.682(3)	0.081(7)
C(131)	1	0.6773(6)	0.962(3)	0.850(3)	0.072(7)
C(132)	1	0.6392(6)	0.027(3)	0.929(2)	0.062(6)
C(133)	1	0.6261(5)	0.976(3)	0.101(2)	0.063(6)
C(134)	1	0.5871(6)	0.013(2)	0.177(2)	0.063(6)
C(135)	1	0.5752(7)	0.965(3)	0.363(3)	0.072(7)
C(136)	1	0.5351(7)	0.005(3)	0.438(3)	0.067(7)
C(137)	1	0.5245(7)	0.951(3)	0.620(2)	0.064(6)
C(138)	1	0.4848(7)	0.998(3)	0.698(3)	0.066(6)
C(139)	1	0.4741(7)	0.952(3)	0.887(3)	0.069(6)
C(140)	1	0.4328(7)	0.993(3)	0.951(3)	0.073(7)
C(141)	1	0.4232(7)	0.937(3)	0.138(3)	0.080(7)
C(142)	1	0.3830(7)	0.985(3)	0.217(3)	0.099(9)
C(143)	1	0.3691(8)	0.919(4)	0.384(4)	0.109(9)
C(144)	1	0.3292(8)	0.969(5)	0.471(4)	0.15(1)
C(145)	1	0.3176(8)	0.885(5)	0.604(5)	0.20(1)
N(2)	1	0.8516(5)	0.351(2)	0.421(2)	0.064(5)
C(200)	1	0.8836(5)	0.254(2)	0.323(2)	0.047(5)
C(201)	1	0.8953(6)	0.326(2)	0.140(2)	0.053(5)
C(202)	1	0.9338(7)	0.257(3)	0.079(2)	0.072(8)
C(203)	1	0.9493(7)	0.319(3)	− 0.102(2)	0.066(6)
C(204)	1	0.9891(6)	0.250(3)	− 0.177(3)	0.077(8)
C(205)	1	0.0010(7)	0.317(3)	− 0.352(3)	0.065(7)
C(206)	1	0.0392(7)	0.247(3)	− 0.425(3)	0.070(7)
C(207)	1	0.0513(8)	0.303(3)	− 0.613(3)	0.080(8)
C(208)	1	0.0908(7)	0.239(3)	− 0.680(3)	0.075(7)
C(209)	1	0.1010(7)	0.304(3)	− 0.860(3)	0.085(9)
C(210)	1	0.1395(7)	0.237(3)	− 0.940(3)	0.079(7)
C(211)	1	0.1523(7)	0.298(3)	− 0.116(3)	0.073(7)
C(212)	1	0.1930(7)	0.252(3)	− 0.182(2)	0.069(6)
C(213)	1	0.2035(7)	0.310(3)	− 0.368(2)	0.084(7)
C(214)	1	0.2433(8)	0.285(4)	− 0.421(3)	0.10(1)
C(215)	1	0.2572(8)	0.336(3)	− 0.616(3)	0.13(1)
C(220)	1	0.8428(6)	0.271(2)	0.593(2)	0.053(5)
C(250)	1	0.8150(6)	0.326(2)	0.333(2)	0.067(6)
C(230)	1	0.8607(6)	0.547(2)	0.511(2)	0.059(6)
C(231)	1	0.8994(6)	0.588(2)	0.635(2)	0.069(6)
C(232)	1	0.9101(7)	0.797(3)	0.670(2)	0.085(8)
C(233)	1	0.9264(7)	0.856(3)	0.478(3)	0.074(7)
C(234)	1	0.9661(7)	0.782(3)	0.411(2)	0.069(7)
C(235)	1	0.9787(8)	0.836(3)	0.231(3)	0.074(7)
C(236)	1	0.0172(6)	0.766(3)	0.152(2)	0.073(6)
C(237)	1	0.0308(8)	0.820(3)	− 0.014(3)	0.080(8)
C(238)	1	0.0700(7)	0.761(3)	− 0.099(3)	0.079(7)
C(239)	1	0.0809(8)	0.813(3)	− 0.269(3)	0.099(9)
C(240)	1	0.1197(8)	0.755(3)	− 0.349(3)	0.096(9)
C(241)	1	0.1342(9)	0.801(4)	− 0.522(3)	0.11(1)
C(242)	1	0.1733(6)	0.752(3)	− 0.597(3)	0.092(9)
C(243)	1	0.1849(8)	0.801(3)	− 0.768(2)	0.101(9)
C(244)	1	0.2260(8)	0.771(3)	− 0.814(3)	0.093(8)
C(245)	1	0.2391(9)	0.814(3)	− 0.004(2)	0.112(9)

parameters, and relevant bond distances and angles are listed in Tables 3, 4, 5, and 6, respectively. The list of the atomic positions of the hydrogens and the structure factors can be obtained from the authors upon request.

The structure of the DHDDMACr compound corresponds to a unit cell of dimensions $a = 34.330(7)$ Å, $b = 7.800(2)$ Å, $c = 7.250(1)$ Å, $\alpha = 103.69(3)^\circ$, $\beta = 89.86(3)^\circ$, $\gamma = 94.12(3)$. During the refinement procedure, three oxygen atoms with full occupancy and eight oxygens with half occupancy were found in the unit cell. The total number of oxygen atom is in good agreement with those expected from density measurement results.

Description of the Crystal Structure

The unit cell contains isolated $(Cr_2O_7)^{2-}$ dichromate clusters which are statistically distributed in layers (Fig. 4a). According to the Cr–O bond distances and the Cr–O–Cr and O–Cr–O bond angles, the dichromate groups may be split into two subunits (Figs. 5(b1) and 5(b2)). Each dichromate ion consists of two $[CrO_4]$ tetrahedra sharing the

TABLE 4
Anisotropic Displacement Parameters (Å²) Values for Nonhydrogen Atoms of $[(C_{16}H_{33})_2(CH_3)_2N]_2Cr_2O_7$ at 293K

Atoms	*U*11	*U*22	*U*33	*U*23	*U*13	*U*12
Cr(1)	0.125(4)	0.053(3)	0.070(3)	0.005(2)	− 0.023(2)	− 0.003(3)
Cr(2)	0.141(4)	0.068(3)	0.049(2)	0.014(2)	− 0.017(2)	− 0.004(3)
O(1)	0.15(2)	0.04(1)	0.01(1)	− 0.03(1)	− 0.06(1)	0.01(1)
O(8)	0.07(1)	0.08(1)	0.00(1)	− 0.051(9)	− 0.02(1)	0.04(1)
O(2)	0.16(1)	0.08(1)	0.10(1)	0.09(1)	− 0.01(1)	0.005(9)
O(6)	0.11(1)	0.059(9)	0.09(1)	0.033(7)	− 0.004(8)	0.017(8)
O(4)	0.07(1)	0.13(2)	0.02(10)	0.020(12)	0.000(9)	0.01(1)
O(5)	0.08(1)	0.13(1)	0.034(8)	0.002(9)	0.000(7)	0.01(1)
O(7)	0.02(1)	0.09(2)	0.21(3)	− 0.06(1)	− 0.02(1)	− 0.03(1)
O(9)	0.04(1)	0.10(1)	0.022(9)	− 0.01(1)	0.010(8)	0.01(1)
O(10)	0.31(4)	0.05(1)	0.12(2)	0.05(1)	0.16(2)	0.16(2)
O(3)	0.06(1)	0.07(2)	0.12(1)	0.02(1)	− 0.00(1)	0.04(1)
O(11)	0.09(1)	0.04(1)	0.028(8)	0.001(8)	0.02(1)	0.01(1)
N(1)	0.017(6)	0.06(1)	0.028(6)	0.018(6)	− 0.008(5)	− 0.01(6)
C(100)	0.06(1)	0.03(1)	0.01(1)	− 0.01(1)	− 0.01(1)	0.01(1)
C(101)	0.06(1)	0.07(1)	0.06(1)	0.04(1)	0.000(9)	0.01(1)
C(102)	0.04(1)	0.05(1)	0.18(2)	− 0.03(1)	− 0.02(1)	0.00(1)
C(103)	0.06(1)	0.04(1)	0.11(1)	0.03(1)	− 0.01(1)	0.00(1)
C(104)	0.06(1)	0.05(1)	0.13(1)	0.01(1)	0.01(1)	0.01(1)
C(105)	0.06(1)	0.07(1)	0.08(1)	0.03(1)	0.00(1)	0.01(1)
C(106)	0.11(1)	0.07(1)	0.06(1)	0.02(1)	− 0.00(1)	− 0.00(1)
C(107)	0.09(1)	0.09(2)	0.07(1)	0.04(1)	0.01(1)	0.01(1)
C(108)	0.11(1)	0.09(1)	0.05(1)	0.03(1)	0.01(1)	0.01(1)
C(109)	0.09(1)	0.09(1)	0.07(1)	0.04(1)	0.01(1)	0.02(1)
C(110)	0.08(1)	0.12(2)	0.05(1)	0.02(1)	0.01(1)	0.00(1)
C(111)	0.08(1)	0.06(1)	0.10(1)	0.02(1)	0.00(1)	0.00(1)
C(112)	0.17(2)	0.11(1)	0.06(1)	0.04(1)	0.02(1)	− 0.01(1)
C(113)	0.08(1)	0.09(1)	0.16(2)	0.03(1)	0.01(1)	0.01(1)
C(114)	0.08(1)	0.24(3)	0.07(1)	0.03(1)	− 0.01(1)	− 0.00(1)
C(115)	0.16(2)	0.21(3)	0.26(3)	0.10(2)	0.11(2)	− 0.00(2)
C(150)	0.09(1)	0.09(1)	0.09(1)	0.08(1)	0.03(1)	0.03(1)
C(120)	0.04(1)	0.12(1)	0.08(1)	0.02(1)	− 0.036(9)	0.01(1)
C(130)	0.08(1)	0.05(1)	0.10(1)	0.00(1)	0.01(1)	0.03(1)
C(131)	0.06(1)	0.10(1)	0.08(1)	0.06(1)	− 0.01(1)	0.01(1)
C(132)	0.06(1)	0.07(1)	0.06(1)	0.01(1)	0.01(1)	0.01(1)
C(133)	0.03(1)	0.08(1)	0.08(1)	0.03(1)	0.00(1)	0.004(9)
C(134)	0.07(1)	0.06(1)	0.05(1)	0.02(1)	0.00(1)	− 0.01(1)
C(135)	0.07(1)	0.08(1)	0.07(1)	0.03(1)	− 0.00(1)	− 0.00(1)
C(136)	0.07(1)	0.07(1)	0.07(1)	0.03(1)	0.01(1)	0.02(1)
C(137)	0.07(1)	0.07(1)	0.06(1)	0.03(1)	0.02(1)	0.02(1)
C(138)	0.07(1)	0.06(1)	0.07(1)	0.03(1)	0.01(1)	0.02(1)
C(139)	0.08(1)	0.05(1)	0.07(1)	0.01(1)	0.01(1)	0.01(1)
C(140)	0.07(1)	0.08(1)	0.07(1)	0.03(1)	0.02(1)	0.01(1)
C(141)	0.06(1)	0.08(1)	0.10(1)	0.02(1)	0.03(1)	0.02(1)
C(142)	0.07(1)	0.13(2)	0.11(1)	0.06(1)	− 0.00(1)	− 0.00(1)
C(143)	0.08(1)	0.09(1)	0.16(2)	0.03(1)	0.04(1)	0.02(1)
C(144)	0.06(1)	0.23(3)	0.16(2)	0.06(2)	0.04(1)	0.00(1)
C(145)	0.07(1)	0.27(4)	0.26(3)	0.09(3)	0.08(1)	0.01(2)
N(2)	0.10(1)	0.05(1)	0.060(9)	0.040(8)	0.016(9)	0.020(9)
C(200)	0.06(1)	0.05(1)	0.05(1)	0.032(9)	− 0.009(9)	− 0.00(1)
C(201)	0.07(1)	0.06(1)	0.043(9)	0.016(8)	0.015(8)	0.027(9)

TABLE 4—*Continued*

Atoms	*U*11	*U*22	*U*33	*U*23	*U*13	*U*12
C(202)	0.09(1)	0.10(1)	0.04(1)	0.04(1)	− 0.00(1)	− 0.00(1)
C(203)	0.10(1)	0.08(1)	0.036(9)	0.04(1)	− 0.001(9)	0.00(1)
C(204)	0.05(1)	0.13(2)	0.06(1)	0.03(1)	0.01(1)	0.04(1)
C(205)	0.06(1)	0.08(1)	0.06(1)	0.03(1)	0.01(1)	0.01(1)
C(206)	0.05(1)	0.08(1)	0.07(1)	0.00(1)	0.01(1)	0.01(1)
C(207)	0.09(1)	0.10(1)	0.05(1)	0.02(1)	− 0.00(1)	− 0.01(1)
C(208)	0.05(1)	0.09(1)	0.07(1)	0.00(1)	0.01(1)	0.00(1)
C(209)	0.06(1)	0.14(2)	0.07(1)	0.06(1)	0.01(1)	− 0.00(1)
C(210)	0.07(1)	0.09(1)	0.07(1)	0.02(1)	− 0.01(1)	− 0.01(1)
C(211)	0.07(1)	0.09(1)	0.06(1)	0.03(1)	− 0.00(1)	0.01(1)
C(212)	0.08(1)	0.08(1)	0.05(1)	0.03(1)	0.01(1)	0.01(1)
C(213)	0.09(1)	0.11(1)	0.06(1)	0.05(1)	0.01(1)	0.00(1)
C(214)	0.09(1)	0.16(2)	0.09(1)	0.08(1)	0.02(1)	0.02(1)
C(215)	0.14(2)	0.19(2)	0.09(1)	0.11(1)	0.05(1)	0.06(1)
C(220)	0.07(1)	0.05(1)	0.034(8)	0.019(8)	0.004(8)	− 0.006(9)
C(250)	0.06(1)	0.06(1)	0.08(1)	0.01(1)	− 0.01(1)	− 0.01(1)
C(230)	0.06(1)	0.06(1)	0.06(1)	0.02(1)	0.01(1)	0.02(1)
C(231)	0.05(1)	0.08(1)	0.06(1)	− 0.011(9)	− 0.016(9)	− 0.01(1)
C(232)	0.16(1)	0.08(1)	0.016(8)	0.022(9)	0.01(1)	0.00(1)
C(233)	0.10(1)	0.07(1)	0.06(1)	0.03(1)	0.01(1)	− 0.00(1)
C(234)	0.08(1)	0.09(1)	0.04(1)	0.03(1)	− 0.00(1)	0.01(1)
C(235)	0.09(1)	0.07(1)	0.06(1)	0.02(1)	− 0.00(1)	0.00(1)
C(236)	0.07(1)	0.09(1)	0.06(1)	0.02(1)	− 0.01(1)	0.02(1)
C(237)	0.07(1)	0.06(1)	0.09(1)	0.00(1)	− 0.00(1)	0.00(1)
C(238)	0.06(1)	0.08(1)	0.09(1)	0.03(1)	− 0.02(1)	− 0.00(1)
C(239)	0.09(1)	0.08(1)	0.11(1)	− 0.01(1)	− 0.00(1)	− 0.01(1)
C(240)	0.10(1)	0.08(1)	0.11(1)	0.03(1)	− 0.03(1)	− 0.00(1)
C(241)	0.11(2)	0.15(2)	0.06(1)	0.01(1)	0.00(1)	− 0.00(1)
C(242)	0.03(1)	0.08(1)	0.14(2)	− 0.01(1)	0.00(1)	0.01(1)
C(243)	0.11(2)	0.16(2)	0.04(1)	0.05(1)	0.01(1)	− 0.02(1)
C(244)	0.10(1)	0.08(1)	0.11(1)	0.03(1)	0.02(1)	0.02(1)
C(245)	0.15(2)	0.14(1)	0.06(1)	0.05(1)	0.01(1)	0.01(1)

bridging oxygen atom O(7) or O(11). As shown in Fig. 5c, the $[CrO_4]$ tetrahedra viewed along the Cr–Cr direction exhibit a staggered conformation: the tetrahedra twist about 49° to 58° (Figs. 5(c1) and 5(c2)) away from the exactly eclipsed conformation in such a way that the ternary symmetry axis disappears. In addition, the O–Cr–O angles subtended at the chromium atoms differ significantly from 109.5° and strongly vary from 92.5° to 124.0° for one dichromate (Table 6). It should be noted that the upper and lower angle values were correlated to the three oxygen atoms (O2, O5, O6) which are common to both dichromates. This probably suggests a small splitting of the undifferentiated oxygen positions which has not been evidenced during the refinement. The distortion of the $[CrO_4]$ tetrahedra is also obvious from the range of Cr–O distances (Table 5). There is a significant and expected difference between the bridging Cr–O(7), Cr–O(11) and nonbridging Cr–O distances with average values of 1.78, 1.68 Å and 1.90, 1.58 Å, for the O(7) and O(11) dichromate subgroups, respectively. These characteristics are in good agreement with the corresponding

TABLE 5
Bond Lengths (Å) in $[(C_{16}H_{33})_2(CH_3)_2N]_2Cr_2O_7$ at 293K

Atoms	Distances (Å)	Atoms	Distances (Å)
Cr(1)–O(1)	1.70(2)	C(138)–C(139)	1.54(3)
Cr(1)–O(3)	1.59(3)	C(139)–C(140)	1.52(3)
Cr(2)–O(4)	1.88(3)	C(140)–C(141)	1.55(3)
Cr(2)–O(7)	1.62(2)	C(141)–C(142)	1.53(4)
Cr(1)–O(7)	1.94(2)	C(142)–C(143)	1.49(3)
		C(143)–C(144)	1.54(4)
Cr(1)–O(2)	1.50(1)	C(144)–C(145)	1.34(4)
Cr(2)–O(5)	1.67(1)		
Cr(2)–O(6)	1.74(1)	N(2)–C(250)	1.39(2)
		N(2)–C(200)	1.46(3)
Cr(1)–O(8)	1.38(2)	N(2)–C(230)	1.52(3)
Cr(1)–O(9)	1.79(2)	N(2)–C(220)	1.54(2)
Cr(2)–O(10)	1.42(2)		
Cr(1)–O(11)	1.92(2)	C(200)–C(201)	1.59(2)
Cr(2)–O(11)	1.88(2)	C(201)–C(202)	1.49(3)
		C(202)–C(203)	1.58(2)
N(1)–C(150)	1.51(2)	C(203)–C(204)	1.56(3)
N(1)–C(100)	1.53(2)	C(204)–C(205)	1.53(3)
N(1)–C(130)	1.55(3)	C(205)–C(206)	1.50(3)
N(1)–C(120)	1.66(2)	C(206)–C(207)	1.57(3)
		C(207)–C(208)	1.52(4)
C(100)–C(101)	1.50(2)	C(208)–C(209)	1.54(3)
C(101)–C(102)	1.42(3)	C(209)–C(210)	1.52(4)
C(102)–C(103)	1.41(3)	C(210)–C(211)	1.52(3)
C(103)–C(104)	1.51(3)	C(211)–C(212)	1.52(3)
C(104)–C(105)	1.52(3)	C(212)–C(213)	1.56(3)
C(105)–C(106)	1.52(3)	C(213)–C(214)	1.43(3)
C(106)–C(107)	1.61(3)	C(214)–C(215)	1.62(3)
C(107)–C(108)	1.50(4)	C(230)–C(231)	1.58(2)
C(108)–C(109)	1.60(3)	C(231)–C(232)	1.60(3)
C(109)–C(110)	1.52(4)	C(232)–C(233)	1.65(3)
C(110)–C(111)	1.55(3)	C(233)–C(234)	1.55(3)
C(111)–C(112)	1.50(4)	C(234)–C(235)	1.51(3)
C(112)–C(113)	1.60(3)	C(235)–C(236)	1.52(3)
C(113)–C(114)	1.50(4)	C(236)–C(237)	1.44(3)
C(114)–C(115)	1.50(3)	C(237)–C(238)	1.54(4)
C(130)–C(131)	1.45(3)	C(238)–C(239)	1.42(3)
C(131)–C(132)	1.50(3)	C(239)–C(240)	1.51(4)
C(132)–C(133)	1.46(2)	C(240)–C(241)	1.46(3)
C(133)–C(134)	1.47(3)	C(241)–C(242)	1.49(4)
C(134)–C(135)	1.53(3)	C(242)–C(243)	1.43(3)
C(135)–C(136)	1.50(3)	C(243)–C(244)	1.47(4)
C(136)–C(137)	1.51(3)	C(244)–C(245)	1.55(3)
C(137)–C(138)	1.51(3)		

symmetry and distances observed for the triclinic $[C_{18}H_{37}(CH_3)_3]_2Cr_2O_7$[22] compound and consistent with the staggering angle observed in the Newman projection, except that in $[(C_{16}H_{33})_2(CH_3)_2N]_2Cr_2O_7$ the Cr–$O_{terminal}$ bond distances are somewhat shorter. The short bond lengths, Cr(1)–O(8) and Cr(2)–O(10), can be attributed to the rotation of dichromate groups around a pseudo-ternary axis which is taken into account by a statistic distribution in the *P*1 space group.

The $(Cr_2O_7)^{2-}$ clusters are arranged in layers and their anionic charge is counterbalanced by those of the dihexadecyldimethylammonium cations. The O–H, O–C, and O–N distances are higher than the sum of the van der Waals radii. Therefore, the $(Cr_2O_7)^{2-}$ clusters are probably in equilibrium with $DHDDMA^+$ thanks to coulombic interactions. The surfactants pack within the crystal so that the lipophilic groups of different molecules are gathered together in a lipophilic region and the hydrophilic groups are similarly arranged within polar regions. As the most common packing structure observed in a crystalline domain, the dihexadecyldimethylammonium chromate adopts a bilayer configuration in which the $DHDDMA^+$ hydrocarbon chains are extended away from the dichromate planes (Fig. 4). In this bilayer resulting from tail to tail pairing, the terminal methyl group planes lie in the center and the polar groups are found on the outside (polar) surface. The opposite ion planes are staggered so as to provide ionic stabilization within the structure. Finally, the layered structure is composed of an alternating arrangement of an inorganic wall, $(Cr_2O_7)^{2-}$, and organic bilayer.

The crystal structure of DHDDMACr is quite similar to that of $[(C_nH_{2n+1})_2(CH_3)_2N]_2Br \cdot H_2O$ with $n = 14$, 18 (28, 29). All the compounds crystallize in triclinic systems and only differ in the space group which is centrosymmetric, $P\bar{1}$, for the latter instead of noncentrosymmetric for the former. According to the *P*1 space group, two amphiphilic molecules should be distinguished and will be noted 2C16N(1) and 2C16N(2) in the following text. The conformational structure of the chains of molecules within surfactant is in first approximation, all-*trans* (linear). The average C–C bond distance and C–C–C bond angle are 1.51 Å and 115.7° for 2C16N(1) and 1.5 Å and 113.5° for 2C16N(2). These values are in good agreement with those previously reported for the long hydrocarbon chains of the amphiphilic compounds (29–31). The isotropic thermal vibration parameters show that the carbon atoms neighboring the ionic layer, constituted by the polar heads and the anionic dichromates, have lower amplitudes of thermal vibration than those located at the far end of the saturated alkyl chains. The *U*eq values gradually increase along the hydrocarbon chain toward the methyl end groups (Table 3). This effect is not unexpected since the motion of these atoms is restrained by the polar head group. So, the high values of the *U*eq observed for the carbon atoms located at the end of the alkyl chains and the short bond length C(144)–C(145) probably result from the beginning of a chain melting phenomenon (conformational disorder of the alkyl chains which really appears in mesophasic domain). To clarify this end point, NMR and IR experiments are actually in progress.

The structure of the amphiphilic molecules in the DHDDMACr crystal is typical of that of ionic dichain surfactants (32). These molecules are usually bent in the vicinity of the polar group in such way that the straight

TABLE 6
Angles (Å^2) in $[(CH_{16}H_{33})_2(CH_3)_2N]_2Cr_2O_7$ at 293K

Atoms	Angles (°)	Atoms	Angles (°)	Atoms	Angles (°)
Cr(2)–O(7)–Cr(1)	133(2)	C(150)–N(1)–C(100)	116(2)	C(250)–N(2)–C(200)	119(2)
				C(250)–N(2)–C(230)	109(2)
O(2)–Cr(1)–O(1)	113(1)	C(150)–N(1)–C(130)	109(2)	C(200)–N(2)–C(230)	117(2)
O(2)–Cr(1)–O(7)	100(1)	C(100)–N(1)–C(130)	111.4(14)	C(250)–N(2)–C(220)	100(2)
O(2)–Cr(1)–O(3)	124(1)	C(150)–N(1)–C(120)	111.3(13)	C(200)–N(2)–C(220)	105.4(14)
O(1)–Cr(1)–O(7)	105(2)	C(100)–N(1)–C(120)	104.3(14)	C(230)–N(2)–C(220)	103.2(14)
O(3)–Cr(1)–O(7)	103(1)	C(130)–N(1)–C(120)	104.3(14)		
O(3)–Cr(1)–O(1)	109(1)			N(2)–C(200)–C(201)	110(2)
O(6)–Cr(2)–O(4)	92.5(1)	C(101)–C(100)–N(1)	117(2)		
O(7)–Cr(2)–O(6)	117(1)			C(202)–C(201)–C(200)	106(2)
O(5)–Cr(2)–O(4)	105.4(8)	C(102)–C(101)–C(100)	119(2)	C(201)–C(202)–C(203)	112(2)
O(7)–Cr(2)–O(4)	102.8(1)	C(101)–C(102)–C(103)	117(2)	C(202)–C(203)–C(204)	115(2)
O(5)–Cr(2)–O(7)	124(1)	C(102)–C(103)–C(104)	116(2)	C(205)–C(204)–C(203)	110(2)
		C(103)–C(104)–C(105)	114(2)	C(204)–C(205)–C(206)	110(2)
O(5)–Cr(2)–O(6)	109.1(9)	C(106)–C(105)–C(104)	114(2)	C(207)–C(206)–C(205)	112(2)
		C(105)–C(106)–C(107)	112(2)	C(206)–C(207)–C(208)	111(2)
O(8)–Cr(1)–O(9)	103(1)	C(108)–C(107)–C(106)	112(2)	C(207)–C(208)–C(209)	108(2)
O(2)–Cr(1)–O(9)	97(1)	C(107)–C(108)–C(109)	112(2)	C(210)–C(209)–C(208)	111(2)
O(8)–Cr(1)–O(11)	118(1)	C(110)–C(109)–C(108)	114(2)	C(209)–C(210)–C(211)	114(2)
O(8)–Cr(1)–O(2)	118(2)	C(109)–C(110)–C(111)	110(2)	C(210)–C(211)–C(212)	114(2)
O(2)–Cr(1)–O(11)	112.3(8)	C(112)–C(111)–C(110)	112(2)	C(211)–C(212)–C(213)	112(2)
O(9)–Cr(1)–O(11)	104(1)	C(111)–C(112)–C(113)	119(2)	C(214)–C(213)–C(212)	113(2)
O(10)–Cr(2)–O(6)	124(1)	C(112)–C(113)–C(114)	121(2)	C(213)–C(214)–C(215)	117(2)
O(6)–Cr(2)–O(11)	97.3(8)	C(115)–C(114)–C(113)	117(3)		
O(10)–Cr(2)–O(5)	120(1)			N(2)–C(230)–C(231)	114(2)
O(10)–Cr(2)–O(11)	108(2)	C(131)–C(130)–N(1)	118(2)		
O(5)–Cr(2)–O(11)	88.3(8)			C(230)–C(231)–C(232)	107(2)
		C(130)–C(131)–C(132)	114(2)	C(233)–C(232)–C(231)	113(2)
Cr(2)–O(11)–Cr(1)	118.9(12)	C(131)–C(132)–C(133)	117(2)	C(234)–C(233)–C(232)	114(2)
		C(134)–C(133)–C(132)	121(2)	C(235)–C(234)–C(233)	111(2)
		C(133)–C(134)–C(135)	119(2)	C(234)–C(235)–C(236)	114(2)
		C(136)–C(135)–C(134)	119(2)	C(237)–C(236)–C(235)	116(2)
		C(135)–C(136)–C(137)	116(2)	C(236)–C(237)–C(238)	119(2)
		C(138)–C(137)–C(136)	116(2)	C(239)–C(238)–C(237)	116(2)
		C(137)–C(138)–C(139)	117(2)	C(238)–C(239)–C(240)	116(3)
		C(140)–C(139)–C(138)	114(2)	C(241)–C(240)–C(239)	121(3)
		C(139)–C(140)–C(141)	111(2)	C(240)–C(241)–C(242)	121(3)
		C(142)–C(141)–C(140)	114(2)	C(241)–C(242)–C(243)	117(2)
		C(143)–C(142)–C(141)	119(2)	C(244)–C(243)–C(242)	113(2)
		C(142)–C(143)–C(144)	120(3)	C(243)–C(244)–C(245)	114(2)
		C(145)–C(144)–C(143)	114(3)		

parts of the chains are unequal in length. In each of the surfactant molecules, 2C16N(1) and 2C16N(2), one of the two alkyl chains is bent at almost right angles at the C(102) and C(232) carbon atoms. In addition, the isotropic thermal motion factors of the two carbons are quite high compared to those of the surrounding carbon atoms. The straight part of both chains have a *trans* zigzag conformation with their zigzag planes parallel to each other. Most of the dihedral angles are within the range of $175^\circ \pm 4$ with the exception of the angles indicated on Figs. 6(1) and 6(2). To achieve stable packing of the alkyl chains in the bilayer structure, the DHDDMA molecules adopt the most simple and compact folding pattern (32). Thus, in each surfactant molecule, the two zigzag planes are arranged in parallel fashion with the shortest intramolecular interactions between the two chains of hydrocarbons of about 4.18 Å separation. One zigzag chain C(130)–$\cdots$–C(145) for N(1) and C(200)–$\cdots$–C(215) for N(2) is translated by three CH_2 units along the chain axis to the other C(103)–$\cdots$–C(115) and C(230)–$\cdots$–C(245). This inequality in the length of two arms is readily accommodated in the crystal by tilting the molecule relative to the polar planes.

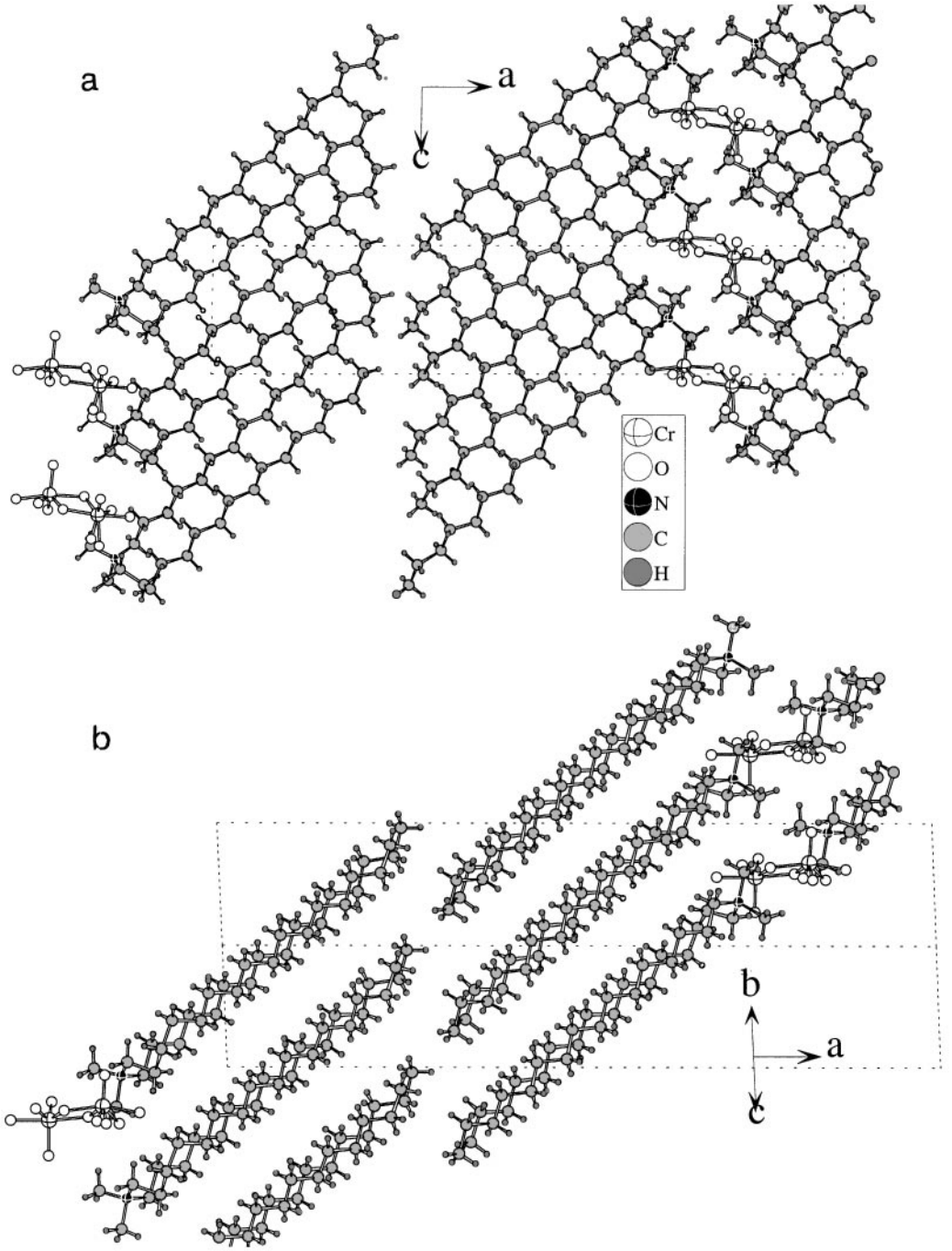

FIG. 4. Packing of $[(C_{16}H_{33})_2(CH_3)_2N]_2Cr_2O_7$ (a) projected onto the *ac*-plane, (b) projected along the (011) direction. The dichromate anions are represented with the 11 oxygen atoms. In between the $(Cr_2O_7)^{2-}$ planes, the DHDDMA chains lay parallel to one another with their dimethylammonium head groups oriented in opposite direction.

The two organic molecules 2C16N(1) and 2C16N(2) of the unit cell are related by centrosymmetry and pack tail–to–tail in a bimolecular layer with tilting of the long hydrocarbon chains. A space filling model of hydrocarbon chains in the *trans* conformation is achieved by using the subcell concept (34). In this approach, the side-by-side packing of the hydrocarbon chains can usually be described by a subcell (35, 36) indicating the translation (c_s) between equivalent positions within the periodic carbon chain and in adjacent chains (a_s and b_s). In DHDDMACr (Fig. 7), the

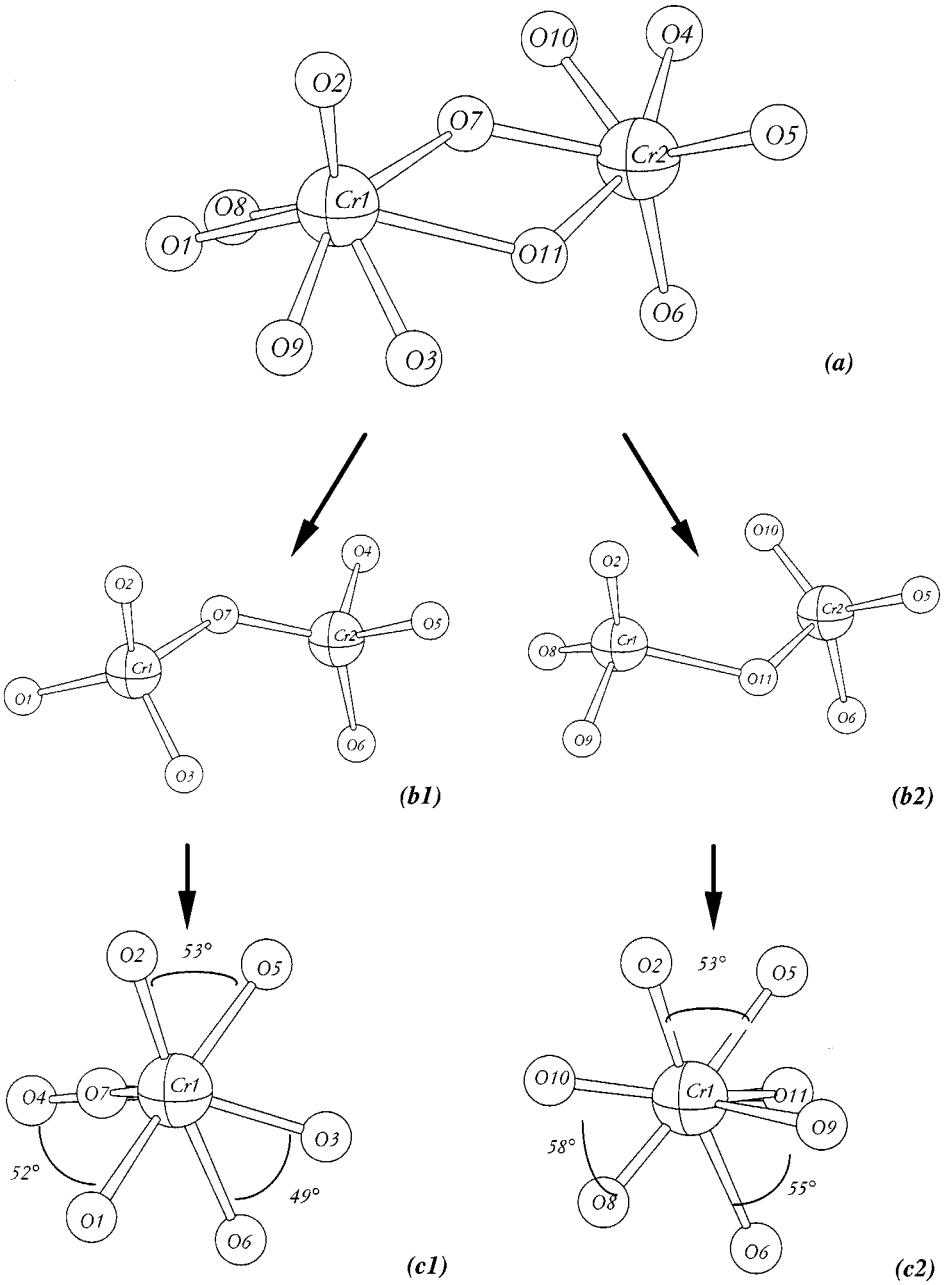

FIG. 5. (a) Dichromate unit represented with the 11 oxygen atoms belonging to the chrome coordination, ((b1), (b2)) the two $(Cr_2O_7)^{2-}$ subunits present in $[(C_{16}H_{33})_2(CH_3)_2N]_2Cr_2O_7$, ((c1), (c2)) projection of the two $(Cr_2O_7)^{2-}$ groups along the Cr–Cr direction showing the torsion angles (°).

alkyl chains pack laterally according to the triclinic packing mode with a subcell $a_s = 7.80$ Å, $b_s = 5.01$ Å, $c_s = 2.57$ Å, $\alpha_s = 90.9°$, $\beta_s = 98.9°$, $\gamma_s = 104.0°$.

The chains axis forms an angle of 46° (angle of tilt) relative to the normal of the plane containing the polar groups which is built up from the polar head of surfactant molecules and dichromate anions. The cross-sectional area of the polar group, which equals 54.9 Å^2 ($b \times c \times \sin\alpha$), is much larger than that of the hydrocarbon chains, which is defined by ($a_s \times b_s \times \sin\gamma_s$) and equals 37.84 Å^2. Therefore, the tilting of 46° ($\cos\varphi = (a_s \times b_s \times \sin\gamma_s)/a \times b \times \sin\gamma = (38/54.9)$) of the alkyl chain takes place so as to accommodate the large area of the hydrophilic part. It is worth noting that the addition of a second alkyl chain compared to the monoalkyled *bis*-hexadecyltrimethylammonium dichromate does not modify the surface area of the polar head but

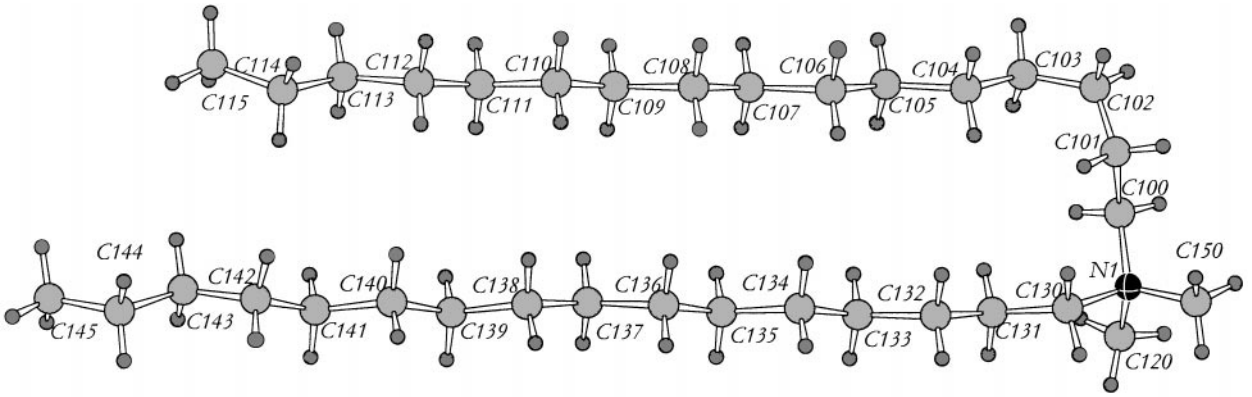

dihedral angles of the 2C16N(1) zigzag part :
N(1)–C(130)–C(131)–C(132)=166°, C(111)–C(112)–C(113)–C(114)=168°,
C(112)–C(113)–C(114)–C(115)=165°,C(140)–C(141)–C(142)–C(143)=167°,
C(141)–C(142)–C(143)–C(144)=156°
dihedral angles of the 2C16N(1) folding part :
C(130)–N(1)–C(100)–C(101)=57°, C(100)–N(1)–C(130)–C(131)=64°,
N(1)–C(100)–C(101)–C(102)=167°,
C(100)–C(101)–C(102)–C(103)=65°, C(101)–C(102)–C(103)–C(104)=64°

(a1)

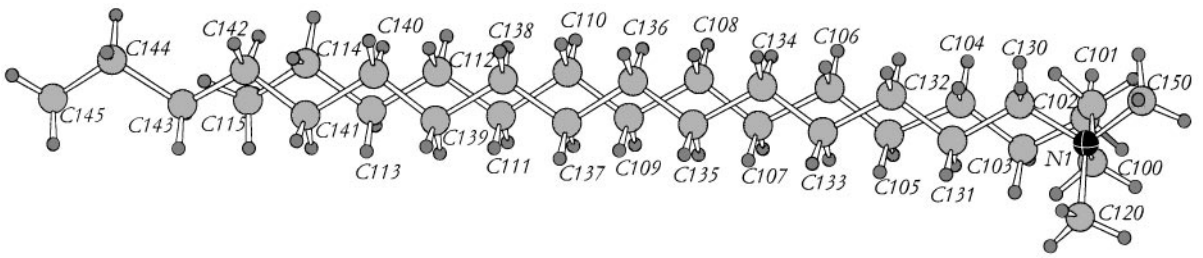

(a2)

FIG. 6. ((a1), (b1)) molecular conformation of the molecules of surfactant ($DHDDMA^+$) in the $[(C_{16}H_{33})_2(CH_3)_2N]_2Cr_2O_7$ and view of their atomic labeling. ((a2), (b2)) molecular conformation of the $(DHDDMA)^+$ molecules viewed along the direction normal to the zigzag plane.

the cross-sectional area of hydrocarbon chains is doubled. Consequently, the tilt angle of the chains relative to the normal of the hydrophilic plane decreases.

CONCLUSION

The new mesostructured $[(C_{16}H_{33})_2(CH_3)_2N]_2Cr_2O_7$ is another example illustrating the templating effect of dihexadecyldimethylammonium on the dichromate groups. The DSC analysis supported by polarizing optical microscopy experiments reveals crystal-to-liquid crystal and liquid crystal-to-liquid phase transitions at $T = 69$ and 141°C, respectively. Inside this temperature range, the DHDDMACr exhibits a typical mosaic texture of a smectic A mesophase. This lamellar character is observed, in crystalline domains, on the XRPD patterns as well. The $[(C_{16}H_{33})_2(CH_3)_2N]_2Cr_2O_7$ crystal structure contains discrete dichromates statistically spread in layers, separated by a double layer of dihexadecyldimethylammonium surfactant. The alkyl chains lie in parallel, and their packing can be described by using the subcell concept in a triclinic system. The tilt angle of about 46° relative to the normal of the polar layer is well approximated by the relation $(\cos\varphi = (a_s \times b_s \times \sin\gamma_s)/a \times b \times \sin\gamma = (38/54.9))$ in which the numerator corresponds to the cross-sectional area of the hydrocarbon chains while the denominator represents the surface area of the polar part.

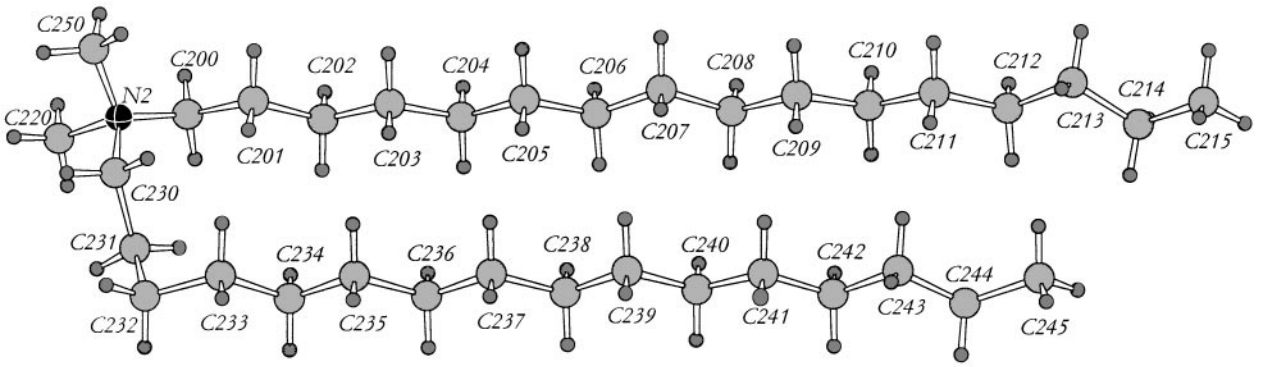

(b1)

dihedral angles of the 2C16N(2) zigzag part :
N(2)–C(200)–C(201)–C(202)=163°, C(241)–C(242)–C(243)–C(244)=168°,
C(211)–C(212)–C(213)–C(214)=155°.
dihedral angles of the 2C16N(2) folding part :
C(230)–N(2)–C(230)–C(231)=56°, C(200)–N(2)–C(230)–C(231)=53°,
N(2)–C(230)–C(231)–C(232)=167°,
C(230)–C(231)–C(232)–C(233)=75°, C(231)–C(232)–C(233)–C(234)=66°.

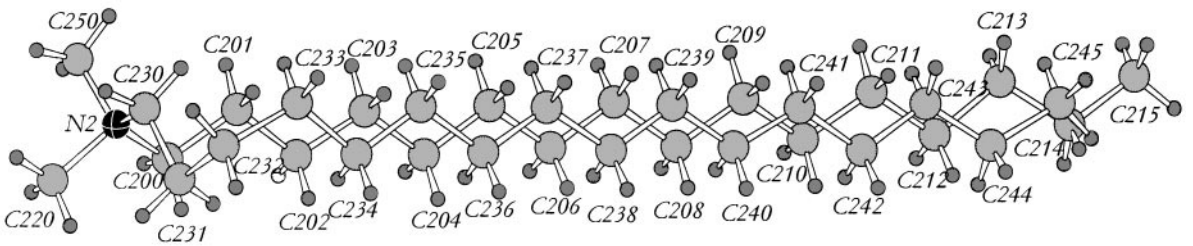

(b2)

FIGURE 6—*Continued*

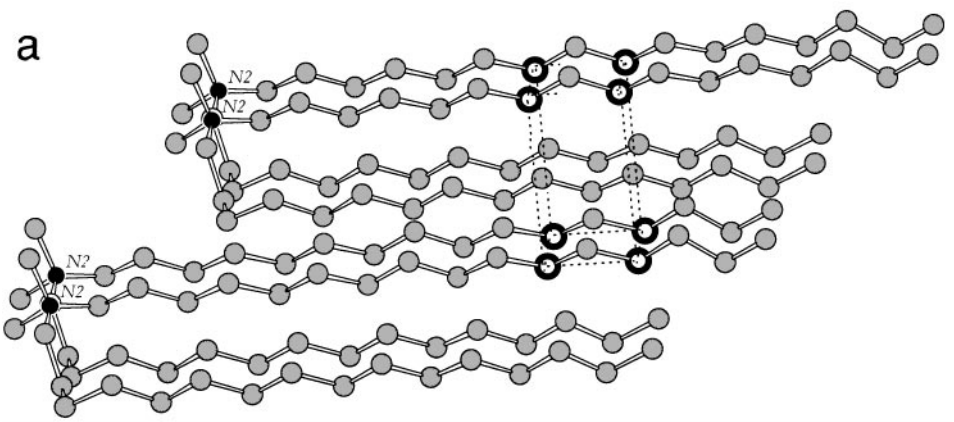

FIG. 7. (a) The arrangement of aliphatic hydrocarbon chains of $[(C_{16}H_{33})_2(CH_3)_2N]_2Cr_2O_7$. The double hydrocarbon chains packing is described by triclinic subcell with a_s, b_s, c_s, α_s, β_s, γ_s parameters. Details of the triclinic subcell are given in (b) and (c).

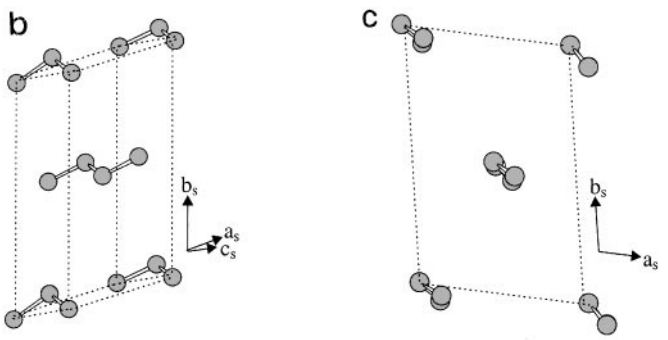

FIGURE 7—*Continued*

REFERENCES

1. T. Kunitake, Y. Okahata, K. Tamaki, F. Kumamaru, and M. Takayanagi, *Chem. Lett*. 367 (1977).
2. T. Kunitake and Y. Okahata, *J. Am. Chem. Soc*. **99,** 3860 (1977).
3. T. Kajiyama, A. Kumano, M. Takayanagi, Y. Okahata, and T. Kunitake, "Contemporary Topics in Polymer Science" (W. J. Bailey and T. Tsuruta, Eds.), Vol. 4, p. 829. Plenum Press, New York, 1984.
4. C. T. Kresge, M. E. Leonowicz, J. C. Vartuli, and J. S. Beck, *Nature* **359,** 710 (1992).
5. J. S. Beck, J. C. Vartuli, W. J. Roth, M. E. Leonowicz, C. T. Kresge, K. D. Schmitt, C. T-W Chu, D. H. Olson, E. W. Sheppard, S. B. McCullen, J. B. Higgins, and J. L. Schlenker, *J. Am. Chem. Soc*. **114,** 10834 (1992).
6. J. C. Vartuli, K. D. Schmitt, C. T. Kresge, W. J. Roth, M. E. Leonowicz, S. B. McCullen, S. D. Hellring, J. S. Beck, J. L. Schlenker, D. H. Olson, and E. W. Sheppard, *Chem. Mater*. **7,** 2317 (1994).
7. J. S. Beck, J. C. Vartuli, G. J. Kennedy, C. T. Kresge, W. J. Roth, and S. E. Schramm, *Chem. Mater*. **6,** 1816 (1994).
8. M. E. Davis, *Chem. Ind*. **17,** 337 (1992).
9. C.-Y. Chen, H.-X. Li, and M. E. Davis, *Microporous Mater*. **2,** 17 (1993).
10. M. E. Davis, *Nature* **364,** 391 (1993).
11. A. Monnier, F. Schüth, Q. Huo, D. Kumar, D. Margolese, R. S. Maxwell, G. D. Stucky, M. Krishnamurty, P. M. Petroff, A. Firouzi, M. Janicke, and B. F. Chmelka, *Science* **261,** 3 (1993).
12. P. T. Tanev, M. Chibwe, and T. J. Pinnavaia, *Nature* **368,** 321 (1994).
13. T. Tanev and T. J. Pinnavaia, *Science* **267,** 865 (1995).
14. S. A. Bagshaw, E. Prouzet, and T. J. Pinnavaia, *Science* **262,** 1242 (1995).
15. G. Fu, C. A. Fyfe, W. Schweiger, and G. T. Kokotailo, *Angew. Chem. Int. Ed. Engl*. **34,** 1499 (1995).
16. A. Chenite, Y. Le Page, and A. Sayari, *Chem. Mater*. **7,** 1015 (1995).
17. Z. Luan, C.-F. Cheng, W. Zhou, and J. Klinowski, *J. Phys. Chem*. **99,** 1018 (1995).
18. A. Sayari, C. Dunamah, and L. Moudrakovski, *Chem. Mater*. **7,** 813 (1995).
19. Q. S. Huo, D. I. Margolese, U. Ciesla, P. Feng, T. E. Gier, P. Sieger, R. Leon, P. M. Petroff, F. Schuff, and G. D. Stucky, *Nature* **368,** 317 (1994).
20. A. Stein, M. Fendorf, T. Jarvie, K. T. Mueller, A. J. Benesi, and T. E. Mallouk, *Chem. Mater*. **7,** 304 (1995).
21. G. G. Janauer, A. D. Dobley, P. Y. Zavalij, and M. S. Whittingham, *Chem. Mater*. **9,** 647 (1997).
22. S. Ayyappan, N. Ulagappan, and C. N. R. Rao, *J. Mater. Chem*. **6,** 1737 (1996).
23. N. Fossé, M. Caldes, O. Joubert, M. Ganne, and L. Brohan; *J. Solid State Chem*. **139,** 310 (1998).
24. J. M. Barbet, M. Evain, P. Deniard, and R. Brec, PROLIX: Treatment of INEL X-RAY curve detector powder diffraction data: chain program and experimental results.
25. SHELXTL VS. Siemens Analytical Instrumentation. Inc., Madison, WI.
26. R. G. Laughin, "The Aqueous Phase Behavior of Surfactants, Colloid Science," Academic Press, San Diego, 1994.
27. M. Evain, U-FIT: A cell parameter refinement program, IMN Nantes, 1992.
28. K. Okuyama, N. Iijima, K. Hirabayashi, T. Kunitake, and M. Kusunoki, *Bull. Chem. Soc. Jpn*. **61,** 2337 (1988).
29. K. Okuyama, Y. Soboi, N. Iijima, K. Hirabayashi, T. Kunitake, and T. Kajiyama, *Bull. Chem. Soc. Jpn*. **61,** 1485 (1988).
30. S. Abrahamsson, B. Dahlen, and I. Pascher, *Acta Cryst. Sect. B* **33,** 2008 (1977).
31. I. Pascher and S. Sundell, *Biochim. Biophys. Acta* **855,** 68 (1986).
32. D. F. Evans and H. Wennerström, "The Colloidal Domain where Physics, Chemistry, Biology, and Technology Meet," Vol. 12, VCH Weinheim/New York, 1994.
33. E. Segerman, *Acta. Cryst*. **19,** 789 (1965).
34. S. Abrahamsson, B. Dahlen, H. Lofgren, and I. Pascher, *Prog. Chem. Fats Other Lipids* **16,** 125 (1978).
35. V. Vand, and I. P. Bell, *Acta. Cryst*. **4,** 465 (1951).
36. E. Von Sydow, *Ark. Kemi*. **9,** 231 (1956).